Neural Network-Based Repetitive Learning Control of Euler Lagrange Systems: An Output Feedback Approach

Enver Tatlicioglu, Necati Cobanoglu, and Erkan Zergeroglu

***Abstract*—In this letter, position tracking control problem of a class of fully actuated Euler Lagrange (EL) systems is aimed. The reference position vector is considered to be periodic with a known period. Only position measurements are available for control design while velocity measurements are not. Furthermore, the dynamic model of the EL systems has parametric and/or unstructured uncertainties which avoid it to be used as part of the control design. To address these constraints, an output feedback neural network-based repetitive learning control strategy is preferred. Via the design of a dynamic model independent velocity observer, the lack of velocity measurements is addressed. To compensate for the lack of dynamic model knowledge, universal approximation property of neural networks is utilized where an online adaptive update rule is designed for the weight matrix. The functional reconstruction error is dealt with the design of a novel repetitive learning feedforward term. The outcome is a dynamic model independent output feedback neural network-based controller with a repetitive learning feedforward component. The stability of the closed–loop system is investigated via rigorous mathematical tools with which semi-global asymptotic stability is ensured.**

***Index Terms*—Nonlinear output feedback, neural networks, Lyapunov methods.**

I. Introduction

EULER Lagrange (EL) systems are utilized for completing some tasks over and over again. In performing periodic tasks, an effective tool is learning controllers that have the advantage of *learning* dynamic model uncertainties with an update rule. Readers are referred to the surveys [1]–[3] or to [4] for more about learning controllers. One line of research on learning controllers was devoted to designing repetitive learning controllers and their modifications. Repetitive learning controllers are mainly used for tracking and/or rejecting periodic signals where their period is known. References [5]–[8] are some of the earlier works in this field. Some extensions were proposed in [9] and [10] mostly to ensure boundedness of the closed–loop system via adding a saturation function to the update laws. By making use of Pade approximation, in [11]–[13], a linearized version of the update law was obtained from the saturation function based one. This yielded linear controllers to be used in conjunction with the learning law but only convergence of the position tracking error to a hyperball at the origin was ensured. In the literature, adaptive methods and especially neural networks were utilized to compensate for some part of the dynamic model uncertainties when controlling EL systems [14], [15]. These methods were also fused with learning controllers [10], [16]. In [10], an adaptive component were used to compensate for the parametric uncertainties in the robot dynamics. And in [16], neural networks were utilized to compensate for some part of the uncertain robot dynamics. While learning controllers were improved with the use of adaptive components all of the above works required knowledge of full–state feedback (i.e., position and velocity sensing are required) for control design.

In this letter, position tracking control of EL systems is considered under the constraints that only position measurements are available and velocity sensing is not and dynamic model is uncertain and thus not to be used as part of the control input. Since periodic reference position vector is to be tracked a repetitive learning control strategy is preferred. To address the lack of velocity sensing an observer based output feedback strategy is employed. And to compensate for the lack of dynamic model knowledge, neural networks are used. The final form of the control input is a dynamic model independent output feedback neural network based controller with a repetitive learning feedforward component. The stability of the closed–loop system is investigated via the use of a novel, four–step Lyapunov based strategy. Firstly, the boundedness of all the closed–loop signals is investigated. Next, the boundedness of the velocity observation error is utilized in obtaining an integral inequality where this result is used in obtaining

Manuscript received March 6, 2017; revised May 17, 2017; accepted June 9, 2017. Date of publication June 28, 2017; date of current version July 21, 2017. This work was supported by the Scientific and Technological Research Council of Turkey under Grant 115E726. Recommended by Senior Editor C. Seatzu. *(Corresponding author: Enver Tatlicioglu.)*

E. Tatlicioglu and N. Cobanoglu are with the Department of Electrical and Electronics Engineering, Izmir Institute of Technology, 35430 Izmir, Turkey (e-mail: enver@iyte.edu.tr; necaticobanoglu@iyte.edu.tr).

E. Zergeroglu is with the Department of Computer Engineering, Gebze Technical University, 41400 Gebze, Turkey (e-mail: e.zerger@gtu.edu.tr).

Digital Object Identifier 10.1109/LCSYS.2017.2720735

an auxiliary non–negative integral function that is later used in the convergence analysis. The stability analysis yields a semi–global asymptotic result.

II. Euler Lagrange System Model and Its Properties

The dynamic model of an n degree of freedom fully actuated Euler Lagrange system is given in the following form [17], [18]

$$M(q)\ddot{q} + V_m(q,\dot{q})\dot{q} + G(q) + F_d\dot{q} = \tau, \tag{1}$$

where $q(t)$, $\dot{q}(t)$, $\ddot{q}(t) \in \mathbb{R}^n$ denote position, velocity, and acceleration vectors, respectively, $M(q) \in \mathbb{R}^{n\times n}$ is the inertia matrix, $V_m(q,\dot{q}) \in \mathbb{R}^{n\times n}$ models the centripetal–Coriolis terms, $G(q) \in \mathbb{R}^n$ includes the gravitational effects, $F_d \in \mathbb{R}^n$ is the constant, diagonal, positive–definite, viscous frictional effects, and $\tau(t) \in \mathbb{R}^n$ is the control torque input. The standard assumption that the left–hand side of (1) being first–order differentiable will be made use of along with the following properties all of which will later be utilized in the controller design and the accompanying stability analysis.

Property 1: The inertia matrix $M(q)$ is positive–definite and symmetric and satisfies the following inequalities [19]

$$m_1 I_n \leq M(q) \leq m_2 I_n, \tag{2}$$

with m_1, $m_2 \in \mathbb{R}$ being known positive bounding constants and $I_n \in \mathbb{R}^{n\times n}$ being the standard identity matrix. Likewise the inverse of $M(q)$ can be bounded as

$$\frac{1}{m_2} I_n \leq M^{-1}(q) \leq \frac{1}{m_1} I_n. \tag{3}$$

Property 2: Following skew–symmetry property is satisfied [19]

$$\xi^T\big(\dot{M} - 2V_m\big)\xi = 0 \ \forall \xi \in \mathbb{R}^n. \tag{4}$$

Property 3: The switching property of the centripetal–Coriolis matrix is satisfied [20]

$$V_m(q,\upsilon)\xi = V_m(q,\xi)\upsilon \ \forall \upsilon, \ \xi, \ \in \mathbb{R}^n. \tag{5}$$

Property 4: Following bounds are valid for the dynamic terms in (1) [9], [20]

$$\|M(\xi) - M(\upsilon)\|_{i\infty} \leq \zeta_{m1}\|\xi - \upsilon\|, \tag{6}$$
$$\left\|M^{-1}(\xi) - M^{-1}(\upsilon)\right\|_{i\infty} \leq \zeta_{m2}\|\xi - \upsilon\|, \tag{7}$$
$$\|V_m(q,\xi)\|_{i\infty} \leq \zeta_{c1}\|\xi\|, \tag{8}$$
$$\|V_m(\xi,w) - V_m(\upsilon,w)\|_{i\infty} \leq \zeta_{c2}\|\xi - \upsilon\|\|w\|, \tag{9}$$
$$\|G(\xi) - G(\upsilon)\| \leq \zeta_g\|\xi - \upsilon\|, \tag{10}$$
$$\|F_d\|_{i\infty} \leq \zeta_f, \tag{11}$$

$\forall \xi, \upsilon, w \in \mathbb{R}^n$, where $\zeta_{m1}, \zeta_{m2}, \zeta_{c1}, \zeta_{c2}, \zeta_g, \zeta_f \in \mathbb{R}$ are positive bounding constants.

The desired form of the Euler Lagrange system dynamics given in (1) can be written

$$\chi_d \triangleq M(q_d)\ddot{q}_d + V_m(q_d,\dot{q}_d)\dot{q}_d + G(q_d) + F_d\dot{q}_d, \tag{12}$$

where $\chi_d(q_d,\dot{q}_d,\ddot{q}_d) \in \mathbb{R}^n$ and q_d, $\dot{q}_d$, $\ddot{q}_d \in \mathbb{R}^n$ denote respectively the desired position, velocity and acceleration.

Property 5: Via utilizing the universal approximation property of neural networks [21]–[23], the term in (12) can be written in the form

$$\chi_d = \phi^T\sigma + \epsilon, \tag{13}$$

where $\phi \in \mathbb{R}^{3n\times n}$ is the constant weight matrix with bounded entries, $\sigma(q_d,\dot{q}_d,\ddot{q}_d) \in \mathbb{R}^{3n}$ is the activation function, and $\epsilon(q_d,\dot{q}_d,\ddot{q}_d) \in \mathbb{R}^n$ is the functional reconstruction error. To ease the notation, let $x_d \triangleq \begin{bmatrix} q_d^T & \dot{q}_d^T & \ddot{q}_d^T \end{bmatrix}^T \in \mathbb{R}^{3n}$. The entries of the functional reconstruction error are bounded via $|\epsilon_i(x_d)| \leq \bar{\epsilon}_i \ \forall i = 1,\ldots,n$ with $\bar{\epsilon}_i$ being positive constants.

III. Control Design

The main aim of the controller design is to ensure tracking of a periodic desired position vector satisfying $q_d(t) = q_d(t-T)$, $\dot{q}_d(t) = \dot{q}_d(t-T)$, $\ddot{q}_d(t) = \ddot{q}_d(t-T)$ for a known period T. There are two constraints that should be dealt with. Firstly, only position measurements are available while velocity measurements are not. Secondly, the terms in the Euler Lagrange dynamics are considered to be uncertain and thus not to be utilized as part of neither the control input torque nor the velocity observer.

The tracking control objective is quantified via the definition of the position tracking error, denoted by $e(t) \in \mathbb{R}^n$, as

$$e \triangleq q_d - q. \tag{14}$$

Let the velocity observation error, shown with $\dot{\tilde{q}}(t) \in \mathbb{R}^n$, is defined as

$$\dot{\tilde{q}} \triangleq \dot{q} - \dot{\hat{q}} \tag{15}$$

and the corresponding position observation error, shown with $\tilde{q}(t) \in \mathbb{R}^n$, being defined in a similar manner as

$$\tilde{q} \triangleq q - \hat{q}, \tag{16}$$

in which $\dot{\hat{q}}(t)$, $\hat{q}(t) \in \mathbb{R}^n$ denote respectively the observed velocity and the corresponding observed position.

To ease the presentation of the rest of the design and analysis, a filtered version of the tracking error, shown with $r(t) \in \mathbb{R}^n$, and a filtered version of velocity observer, shown with $s(t) \in \mathbb{R}^n$, are defined as

$$r \triangleq \dot{e} + \alpha e, \tag{17}$$
$$s \triangleq \dot{\tilde{q}} + \alpha\tilde{q} \tag{18}$$

where $\alpha \in \mathbb{R}$ is a positive constant control gain.

Motivated by the subsequently presented stability analysis, the velocity observer is designed as

$$\dot{\hat{q}} = p + K_0\tilde{q} - K_c e, \tag{19}$$
$$\dot{p} = K_1 \mathrm{Sgn}(\tilde{q}) + K_2\tilde{q} - \alpha K_c e \tag{20}$$

with $p(t) \in \mathbb{R}^n$, K_0, K_c, K_1, $K_2 \in \mathbb{R}^{n\times n}$ being positive–definite, diagonal gain matrices, and $\mathrm{Sgn}(\varsigma) = \begin{bmatrix} \mathrm{sgn}(\varsigma_1) & \cdots & \mathrm{sgn}(\varsigma_n) \end{bmatrix}^T \in \mathbb{R}^n \ \forall \varsigma \in \mathbb{R}^n$. Also motivated by the subsequently presented stability analysis, the control input torque $\tau(t)$ is designed as

$$\tau = \hat{\phi}^T\sigma + \hat{\epsilon} + K_p e + K_c\alpha\big(q_d - \hat{q}\big) + K_c\Big(\dot{q}_d - \dot{\hat{q}}\Big) \tag{21}$$

where $K_p \in \mathbb{R}^{n\times n}$ is a positive–definite, diagonal gain matrix, $\hat{\phi}(t) \in \mathbb{R}^{3n\times n}$ is the estimated weight matrix generated online via

$$\hat{\phi} = k_{nn}\Big(\sigma(t)e^T(t) - \sigma(0)e^T(0) - \int_0^t (\dot{\sigma}(\nu) - \alpha\sigma(\nu))e^T(\nu)d\nu\Big) \tag{22}$$

in which k_{nn} is a constant gain and the feedforward learning term $\hat{\epsilon}(t) \in \mathbb{R}^n$ is obtained from

$$\hat{\epsilon}(t) = \mathrm{Sat}_{\bar{\epsilon}}\big(\hat{\epsilon}(t-T)\big) + k_l\alpha\big(q_d - \hat{q}\big) + k_l\Big(\dot{q}_d - \dot{\hat{q}}\Big) \tag{23}$$

where $k_l \in \mathbb{R}$ is a positive constant gain, $\bar{\epsilon} \triangleq \big[\,\bar{\epsilon}_1 \ \cdots \ \bar{\epsilon}_n\,\big] \in \mathbb{R}^n$ denotes the limits of the vector saturation function $\mathrm{Sat}_{\bar{\epsilon}}(\cdot) \in \mathbb{R}^n$ whose entries are defined as

$$\mathrm{sat}_{\bar{\epsilon}_i}\big(\hat{\epsilon}_i\big) = \begin{cases} \bar{\epsilon}_i \mathrm{sgn}\big(\hat{\epsilon}_i\big), & \big|\hat{\epsilon}_i\big| > \bar{\epsilon}_i \\ \hat{\epsilon}_i, & \big|\hat{\epsilon}_i\big| \le \bar{\epsilon}_i \end{cases} \tag{24}$$

To ensure boundedness a projection algorithm such as the one in [24] is considered to be utilized at the right hand side of (22). It is noted that

$$q_d - \hat{q} = e + \tilde{q}, \tag{25}$$

$$\dot{q}_d - \dot{\hat{q}} + \alpha\big(q_d - \hat{q}\big) = r + s \tag{26}$$

using which the controller of (21) and the feedforward learning term of (23) are written as

$$\tau = \hat{\phi}^T\sigma + \hat{\epsilon} + K_p e + K_c(r+s), \tag{27}$$

$$\hat{\epsilon}(t) = \mathrm{Sat}_{\bar{\epsilon}}\big(\hat{\epsilon}(t-T)\big) + k_l(r+s). \tag{28}$$

It is highlighted that the controller along with the feedforward learning term designed above does not require velocity measurements but for the ease of the presentation in the rest of this letter, the formulations in (27) and (28) will be made use of rather than their implementable versions.

A. Observer Error Dynamics

To obtain the observer error dynamics, the time derivative of (18) is taken first, then (19), (27), (28) are inserted, next K_0 is designed as

$$K_2 = \alpha(K_0 - \alpha I_n), \tag{29}$$

and finally performing simplifications yields

$$\dot{s} = N_d + N_b - K_1\mathrm{Sgn}(\tilde{q}) + K_c r - \frac{1}{\alpha}K_2 s, \tag{30}$$

in which $N_d(q, q_d, \dot{q}_d, \ddot{q}_d, t) \in \mathbb{R}^n$ and $N_b(q, \dot{q}, q_d, \dot{q}_d, e, r, s, t) \in \mathbb{R}^n$ are defined as

$$N_d \triangleq \ddot{q}_d + M^{-1}(q)\Big[\mathrm{Sat}_{\bar{\epsilon}}\big(\hat{\epsilon}(t-T)\big) - \epsilon(t) + \tilde{\phi}^T\sigma\Big], \tag{31}$$

$$\begin{aligned} N_b \triangleq &\Big[M^{-1}(q) - M^{-1}(q_d)\Big]M(q_d)\ddot{q}_d \\ &+ M^{-1}(q)\big[V_m(q_d, \dot{q}_d)\dot{q}_d - V_m(q, \dot{q})\dot{q} \\ &+ G(q_d) - G(q) + F_d\dot{e} + K_p e \\ &+ K_c(r+s) + k_l(r+s)\big]. \end{aligned} \tag{32}$$

Applying (3), (6)–(11) to N_d and N_b yields the following bounds

$$\|N_d\| \le \zeta_d, \tag{33}$$

$$\|N_b\| \le \rho_1\|e\| + \rho_2\|r\| + \rho_3\|s\| + \rho_4\|r\|^2 \tag{34}$$

where $\zeta_d,\ \rho_1,\ \rho_2,\ \rho_3,\ \rho_4 \in \mathbb{R}$ are positive known bounding constants (readers are referred [25] for the details of upper bounds).

B. Tracking Error Dynamics

To obtain the tracking error dynamics, the time derivative of $r(t)$ is taken first, then pre–multiplied by $M(q)$, and next (1), (14), (21) are utilized to obtain

$$M\dot{r} = -V_m r + \tilde{\chi} + \tilde{\phi}^T\sigma + \tilde{\epsilon} - K_p e - K_c(r+s), \tag{35}$$

in which $\tilde{\epsilon}(t) \triangleq \epsilon - \hat{\epsilon} \in \mathbb{R}^n$, $\tilde{\phi}(t) \triangleq \phi - \hat{\phi} \in \mathbb{R}^{3n\times n}$ and $\tilde{\chi}(t) \in \mathbb{R}^n$ is defined as

$$\tilde{\chi} \triangleq M(\ddot{q}_d + \alpha\dot{e}) + V_m(\dot{q}_d + \alpha e) + G + F_d\dot{q} - \chi_d \tag{36}$$

which can be bounded as [25]

$$\|\tilde{\chi}(t)\| \le (\zeta_1 + \zeta_2\|e\|)\|e\| + (\zeta_3 + \zeta_4\|e\|)\|r\| \tag{37}$$

with $\zeta_1,\ \zeta_2,\ \zeta_3,\ \zeta_4 \in \mathbb{R}$ being known positive bounding constants.

IV. Stability Analysis

In view of the closed–loop error dynamics in (30) and (35), following theorem is introduced to analyze the stability of position tracking error and velocity observation error.

Theorem 1: The velocity observer in (19), (20) and the control law in (21) with the feedforward learning term in (23) and the neural network weight update in (22) guarantee the closed–loop system to be semi–globally asymptotically stable in the sense that

$$\|e(t)\|,\ \Big\|\dot{\tilde{q}}(t)\Big\| \to 0 \text{ as } t \to 0 \tag{38}$$

provided that the observer gain is selected to satisfy (29), the controller gain K_p is chosen to satisfy $\lambda_{\min}\{K_p\} \ge \frac{1}{\alpha}$, the controller gain K_c is designed as

$$K_c = \Big(k_d\zeta_1^2 + k_d\zeta_2^2 + \zeta_3 + k_d\zeta_4^2 + 1\Big)I_n, \tag{39}$$

and the observer gain K_2 is designed as

$$K_2 = \alpha\bigg(k_d\rho_1^2 + k_d\rho_2^2 + \rho_3 + k_d\rho_4^2 + \frac{k_l}{2} + 1\bigg)I_n \tag{40}$$

where k_d is a positive damping constant.

Proof: The proof is conducted in four steps where first a boundedness analysis is performed whose result yields a lemma from which an inequality is obtained which is then used to ensure non–negativeness of an integral term as part of the convergence analysis.

Firstly, a non–negative function, denoted by $V_b(y) \in \mathbb{R}$, is defined as

$$V_b \triangleq \frac{1}{2}r^T M r + \frac{1}{2}e^T K_p e + \frac{1}{2}s^T s, \tag{41}$$

which is bounded as

$$\lambda_1\|y\|^2 \leq V_b \leq \lambda_2\|y\|^2 \tag{42}$$

where $y \triangleq \begin{bmatrix} e^T & r^T & s^T \end{bmatrix}^T$, $\lambda_1 \triangleq \frac{1}{2}\min\{m_1, \lambda_{\min}\{K_p\}, 1\}$, $\lambda_2 \triangleq \frac{1}{2}\max\{m_2, \lambda_{\max}\{K_p\}, 1\}$ in which $\lambda_{\min}\{\cdot\}$ and $\lambda_{\max}\{\cdot\}$ denote respectively minimum and maximum eigenvalues of a matrix.

After taking the time derivative of V_b and substituting for (17), (30) and (35), results in

$$\begin{aligned}\dot{V}_b = r^T\Big[&-V_m r + \tilde{\chi} + \tilde{\phi}^T\sigma + \tilde{\epsilon} - K_p e \\ &- K_c(r+s)\Big] + \frac{1}{2}r^T\dot{M}r + e^T K_p(r - \alpha e) \\ &+ s^T\left[N_d + N_b - K_1\mathrm{Sgn}(\tilde{q}) + K_c r - \frac{1}{\alpha}K_2 s\right],\end{aligned} \tag{43}$$

from which, after canceling common terms, then substituting (28), making use of the bounds in (33), (34), (37), bound of the functional reconstruction error in Property 5, boundedness of the projection algorithm along with the fact that the outputs of saturation and signum functions being bounded, then substituting (39) and (40), and finally making use of the nonlinear damping argument in [24], following is obtained

$$\dot{V}_b \leq -\kappa_1 V_b + \kappa_2 \tag{44}$$

where κ_1 and κ_2 are positive constants (with κ_2 depending on the bounds of $\|\tilde{\phi}^T\sigma\|$, $\|\mathrm{Sat}_{\bar{\epsilon}}(\hat{\epsilon}(t-T))\| \leq \|\bar{\epsilon}\|$, $\|\epsilon(t)\| \leq \|\bar{\epsilon}\|$, $\|N_d(t)\| \leq \zeta_d$, $\|K_1\|_{i\infty} \leq \lambda_{\max}\{K_1\}$). From (41) and (44), $V_b(y) \in \mathcal{L}_\infty$ and thus $e(t)$, $r(t)$, $s(t) \in \mathcal{L}_\infty$. Linear signal chasing tools are applied to show the boundedness of all the remaining signals under the closed–loop operation, including $\tilde{q}(t)$ and $\dot{\tilde{q}}(t)$.

Following lemma of [26] is essential for the next step of the proof.

Lemma 1: Provided the boundedness of $\tilde{q}(t)$ and $\dot{\tilde{q}}(t)$, following inequality can be obtained for the upper bound of the integral of the absolute value of the i^{th} entry of $\dot{\tilde{q}}(t)$

$$\int_{t_0}^{t}\left|\dot{\tilde{q}}_i(\nu)\right|d\nu \leq \gamma_1 + |\tilde{q}_i(t)| + \gamma_2\int_{t_0}^{t}|\tilde{q}_i(\nu)|d\nu, \tag{45}$$

with γ_1 and γ_2 being positive constants.

Following lemma of [27] will be utilized in the convergence analysis part of the proof.

Lemma 2: Provided the entries of the control gain matrix K_1 are chosen to be greater than the upper bound of the auxiliary term $\bar{N}_d(t) \triangleq N_d + \mathrm{Sat}_{\bar{\epsilon}}(\hat{\epsilon}(t-T)) - \epsilon(t) \in \mathbb{R}^n$, following scalar term

$$P \triangleq \zeta_p - \int_0^t s^T(\nu)\big[\bar{N}_d(\nu) - K_1\mathrm{Sgn}(\tilde{q}(\nu))\big]d\nu \tag{46}$$

is non–negative where ζ_p is a positive constant.

To analyze the convergence of the tracking error and the velocity observation error, following non–negative function, denoted by $V_c(t) \in \mathbb{R}$, is introduced

$$\begin{aligned}V_c \triangleq\ & V_b + P + \frac{1}{2k_{nn}}\mathrm{tr}\{\tilde{\phi}^T\tilde{\phi}\} \\ &+ \frac{1}{2k_l}\int_{t-T}^{t}\left\|\mathrm{Sat}_{\bar{\epsilon}}(\epsilon(\nu)) - \mathrm{Sat}_{\bar{\epsilon}}(\hat{\epsilon}(\nu))\right\|^2 d\nu.\end{aligned} \tag{47}$$

The time derivative of (47) is

$$\begin{aligned}\dot{V}_c =\ & \frac{1}{2}r^T\dot{M}r + r^T M\dot{r} + e^T K_p\dot{e} + s^T\dot{s} \\ &- s^T\big[\bar{N}_d - K_1\mathrm{Sgn}(\tilde{q})\big] + \frac{1}{k_{nn}}\mathrm{tr}\{\tilde{\phi}^T\dot{\tilde{\phi}}\} \\ &+ \frac{1}{2k_l}\left\|\mathrm{Sat}_{\bar{\epsilon}}(\epsilon(t)) - \mathrm{Sat}_{\bar{\epsilon}}(\hat{\epsilon}(t))\right\|^2 \\ &- \frac{1}{2k_l}\left\|\mathrm{Sat}_{\bar{\epsilon}}(\epsilon(t-T)) - \mathrm{Sat}_{\bar{\epsilon}}(\hat{\epsilon}(t-T))\right\|^2,\end{aligned} \tag{48}$$

to which after substituting (17), the time derivative of (22), (30), (35), making use of (4), and then canceling common terms yield

$$\begin{aligned}\dot{V}_c =\ & r^T\left(\tilde{\chi} + \tilde{\phi}^T\sigma - K_c r\right) - \alpha e^T K_p e \\ &+ s^T\left(N_b - \frac{1}{\alpha}K_2 s\right) - \mathrm{tr}\{\tilde{\phi}^T\sigma r^T\} \\ &+ \frac{1}{2k_l}\left\|\mathrm{Sat}_{\bar{\epsilon}}(\epsilon(t)) - \mathrm{Sat}_{\bar{\epsilon}}(\hat{\epsilon}(t))\right\|^2 - \frac{1}{2k_l}\|\tilde{\epsilon}(t)\|^2 \\ &+ k_l(r+s)^T s - \frac{k_l}{2}\|r+s\|^2\end{aligned} \tag{49}$$

where $\mathrm{Sat}_{\bar{\epsilon}}(\epsilon(t-T)) - \mathrm{Sat}_{\bar{\epsilon}}(\hat{\epsilon}(t-T)) = \tilde{\epsilon}(t) + k_l(r+s)$ was utilized as well. Following relationship of [10] is essential for the rest of the convergence analysis

$$\left\|\mathrm{Sat}_{\bar{\epsilon}}(\epsilon(t)) - \mathrm{Sat}_{\bar{\epsilon}}(\hat{\epsilon}(t))\right\|^2 - \|\tilde{\epsilon}\|^2 \leq 0. \tag{50}$$

Substituting (34), (37), (39), (40), then making use of (50) and the property of trace operator that $\mathrm{tr}\{\tilde{\phi}^T\sigma r^T\} = r^T\tilde{\phi}^T$ along with (49) yield

$$\begin{aligned}\dot{V}_c \leq\ & -\alpha\lambda_{\min}\{K_p\}\|e\|^2 - \|r\|^2 - \frac{k_l}{2}\|r\|^2 - \|s\|^2 \\ &+ \zeta_1\|r\|\|e\| - k_d\zeta_1^2\|r\|^2 \\ &+ \zeta_2\|r\|\|e\|^2 - k_d\zeta_2^2\|r\|^2 \\ &+ \zeta_4\|r\|^2\|e\| - k_d\zeta_4^2\|r\|^2 \\ &+ \rho_1\|s\|\|e\| - k_d\rho_1^2\|s\|^2 \\ &+ \rho_2\|s\|\|r\| - k_d\rho_2^2\|s\|^2 \\ &+ \rho_4\|s\|\|r\|^2 - k_d\rho_4^2\|s\|^2,\end{aligned} \tag{51}$$

with which utilizing the nonlinear damping argument in [24] gives

$$\begin{aligned}\dot{V}_c \leq\ & -\alpha\lambda_{\min}\{K_p\}\|e\|^2 - \|r\|^2 - \frac{k_l}{2}\|r\|^2 - \|s\|^2 \\ &+ \frac{1}{4k_d}\|e\|^2 + \frac{1}{4k_d}\|e\|^4 + \frac{1}{4k_d}\|e\|^2\|r\|^2 \\ &+ \frac{1}{4k_d}\|e\|^2 + \frac{1}{4k_d}\|r\|^2 + \frac{1}{4k_d}\|r\|^4,\end{aligned} \tag{52}$$

from which is possible to upper bound the right–hand side as

$$\dot{V}_c \leq -\left[1 - \frac{1}{2k_d} - \frac{1}{2k_d}\|y\|^2\right]\|y\|^2 \leq -\kappa_3\|y\|^2 \tag{53}$$

where $\kappa_3 \in \mathbb{R}$ is some positive constant ($0 < \kappa_3 \leq 1$). Integrating (53) in time from initial time to infinity gives that $y(t)$ is square integrable. Since from the first part of the proof boundedness of $y(t)$ and its time derivative was guaranteed, then Barbalat's Lemma [24] can be utilized to prove semi–global asymptotic convergence of the velocity estimation error and the tracking error to the origin. ■

V. SIMULATION RESULTS

To illustrate the performance of the designed controller, a numerical simulation was performed with the model of a two link, planar robot manipulator. The dynamic model in (1) with additive disturbance term τ_d is considered with the following functions

$$M = \begin{bmatrix} p_1 + 2p_3c_2 & p_2 + p_3c_2 \\ p_2 + p_3c_2 & p_2 \end{bmatrix} \tag{54}$$

$$V_m = \begin{bmatrix} -p_3s_2\dot{q}_2 & -p_3s_2(\dot{q}_1 + \dot{q}_2) \\ p_3s_2\dot{q}_1 & 0 \end{bmatrix} \tag{55}$$

$$G = \begin{bmatrix} 0.5m_1gl_1c_1 + m_2g(l_1c_1 + 0.5l_2c_{12}) \\ 0.5m_2gl_2c_{12} \end{bmatrix} \tag{56}$$

$$F_d = \begin{bmatrix} 5.3\dot{q}_1 \\ 1.1\dot{q}_2 \end{bmatrix} \tag{57}$$

$$\tau_d = 0.1\begin{bmatrix} \sin(0.2\pi t) \\ \cos(0.2\pi t) \end{bmatrix} \tag{58}$$

in which $c_1 = \cos(q_1)$, $s_2 = \sin(q_2)$, $c_2 = \cos(q_2)$, $c_{12} = \cos(q_1 + q_2)$, and $p_1 = 3.473$, $p_2 = 0.193$, $p_3 = 0.242$, $m_1 = 3.6$, $m_2 = 2.6$, $l_1 = 0.4$, $l_2 = 0.36$, $g = 9.8$. We would like to note that the above dynamic model is not utilized in the control design when performing the numerical simulations.

The periodic desired joint space trajectory was selected as

$$q_d = \begin{bmatrix} 0.3+\sin(0.2\pi t) \\ 0.3+\sin(0.2\pi t) \end{bmatrix}. \tag{59}$$

The robot manipulator is considered to be at rest with the initial joint position as $q(0) = [0.1, 0.1]^T$rad. Satisfactory tracking performance is obtained when the gains were set as $K_p = 20I_2$, $K_c = 2I_2$, $K_0 = 100I_2$, $K_1 = 5I_2$, $\alpha = 0.1$, $k_{nn} = 100$, $k_L = 0.01$, and the limits of the saturation function were chosen as ± 1. Hyperbolic tangent function is used for the activation function of the neural–network. When choosing the gains, following the linear system convention, the observer gains are chosen bigger to achieve velocity observation first and then the control gains were chosen.

The results of the numerical simulation are presented in Figures 1, 2, 3. In Figure 1, the joint space tracking error $e(t)$ is shown. Position observation error $\tilde{q}(t)$ is presented in Figure 2. Control input torque is given in Figure 3. From Figure 1, it is clear that the joint tracking objective was successfully met and from Figure 2, the joint velocity observation objective was successfully met. And from Figure 1, it can be observed that the proposed repetitive learning controller ensures an improvement on the joint space tracking error in every period of the desired joint trajectory.

Additional numerical simulations were performed by removing the learning component $\hat{\varepsilon}(t)$ or the neural network component from the control input in (21). The tracking error and the velocity observation error were observed to be driven to zero. Square of the integral of the norm of the tracking error (i.e., $\int \|e(\nu)\|^2 d\nu$) and the control input (i.e., $\int \|\tau(\nu)\|^2 d\nu$) were calculated and recorded as performance measures and

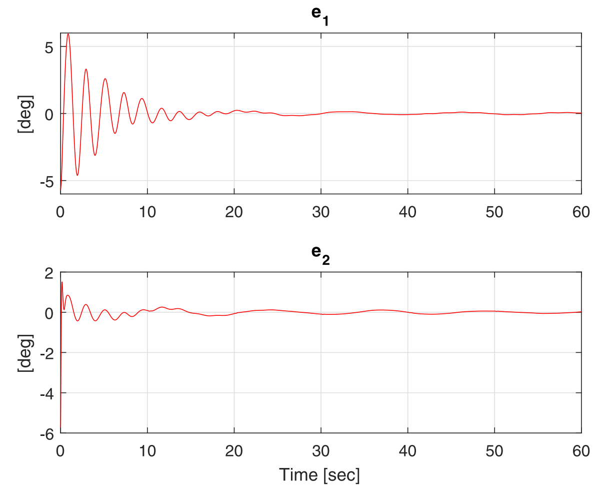

Fig. 1. Joint position tracking error $e(t)$.

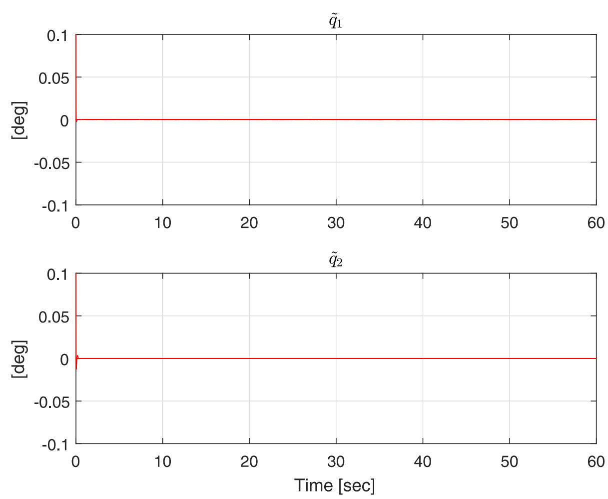

Fig. 2. Auxiliary position observation error $\tilde{q}$.

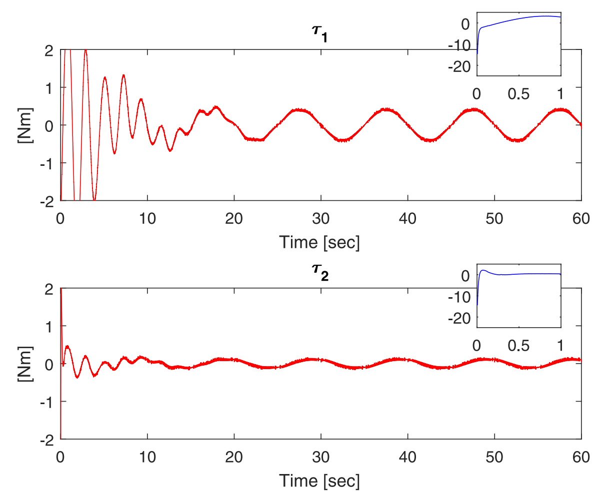

Fig. 3. Control input torque $\tau(t)$.

are presented in Table I. From Table I, it is observed that when the learning component is removed a slightly more amount of control input yielded more tracking error while on the other hand removing the neural network component

TABLE I
PERFORMANCE MEASURES

	$\int \|e(\nu)\|^2 d\nu$	$\int \|\tau(\nu)\|^2 d\nu$
The control input in (21)	56.93	31.17
Without $\hat{\epsilon}(t)$	57.21	31.22
Without $\hat{\phi}^T(t)\sigma(t)$	126.40	21.40

yielded more tracking error. This demonstrates that the design objective is met in the sense that neural network has compensated for most of the modeling uncertainties and the learning component compensated for the functional reconstruction error where in [10] a bigger k_L was required as the learning component had to compensate for all the modeling uncertainties.

VI. CONCLUSION

In this letter, design of a velocity observer based output feedback neural network controller with a repetitive learning feedforward term was presented for tracking control of EL systems. Via a novel four–step Lyapunov type stability analysis, semi–global asymptotic tracking and velocity observation was ensured. While in this letter tracking of a periodic reference position vector was presented a possible important application of the proposed control strategy is for control of active magnetic bearings [28] or atomic force microscopy [29] where the control problem is to reject periodic disturbance type effects (rather than following a periodic reference trajectory). It is our sincere belief that the proposed strategy can with some effort be applicable to address this important research problem.

Note that the system equation considered in this letter does not contain additive disturbance terms. When external disturbance terms are present, the proposed stability analysis would not be able ensure asymptotic convergence of the tracking error signal to zero but at best, to an ultimate bound around the origin. Future work will concentrate on the disturbance rejection properties of the proposed controller. Additionally robustness to the mismatch in the period and dealing with time–varying period are also possible extensions to the proposed work.

REFERENCES

[1] G. Hillerstrom and K. Walgama, "Repetitive control theory and applications—A survey," in *Proc. IFAC World Congr.*, San Francisco, CA, USA, 1996, pp. 1–6.

[2] D. A. Bristow, M. Tharayil, and A. G. Alleyne, "A survey of iterative learning control," *IEEE Control Syst. Mag.*, vol. 26, no. 3, pp. 96–114, Jun. 2006.

[3] Y. Wang, F. Gao, and F. J. Doyle, III, "Survey on iterative learning control, repetitive control, and run-to-run control," *J. Process Control*, vol. 19, no. 10, pp. 1589–1600, 2009.

[4] J.-X. Xu and Y. Tan, *Linear and Nonlinear Iterative Learning Control*. Berlin, Germany: Springer-Verlag, 2003.

[5] S. Hara, Y. Yamamoto, T. Omata, and M. Nakano, "Repetitive control system: A new type servo system for periodic exogenous signals," *IEEE Trans. Autom. Control*, vol. 33, no. 7, pp. 659–668, Jul. 1988.

[6] M. C. Tsai, G. Anwar, and M. Tomizuka, "Discrete time repetitive control for robot manipulators," in *Proc. IEEE Int. Conf. Robot. Autom.*, Philadelphia, PA, USA, 1988, pp. 1341–1347.

[7] W. Messner, R. Horowitz, W.-W. Kao, and M. Boals, "A new adaptive learning rule," *IEEE Trans. Autom. Control*, vol. 36, no. 2, pp. 188–197, Feb. 1991.

[8] R. Horowitz, "Learning control of robot manipulators," *ASME J. Dyn. Syst. Meas. Control*, vol. 115, pp. 402–411, Jun. 1993.

[9] N. Sadegh and R. Horowitz, "Stability and robustness analysis of a class of adaptive controllers for robotic manipulators," *Int. J. Robot. Res.*, vol. 9, no. 3, pp. 74–92, 1990.

[10] W. E. Dixon, E. Zergeroglu, D. M. Dawson, and B. T. Kostic, "Repetitive learning control: A Lyapunov-based approach," *IEEE Trans. Syst., Man, Cybern. B, Cybern.*, vol. 32, no. 4, pp. 538–545, Aug. 2002.

[11] P. Tomei and C. M. Verrelli, "Linear repetitive learning controls for nonlinear systems by Padé approximants," *Int. J. Adapt. Control Signal Process.*, vol. 29, no. 6, pp. 783–804, 2015.

[12] C. M. Verrelli, "Repetitive learning control design and period uncertainties," *Asian J. Control*, vol. 17, no. 6, pp. 2417–2426, 2015.

[13] S. Scalzi, S. Bifaretti, and C. M. Verrelli, "Repetitive learning control design for LED light tracking," *IEEE Trans. Control Syst. Technol.*, vol. 23, no. 3, pp. 1139–1146, May 2015.

[14] F. L. Lewis, "Nonlinear network structures for feedback control," *Asian J. Control*, vol. 1, no. 4, pp. 205–228, 1999.

[15] Y. H. Kim, F. L. Lewis, and D. M. Dawson, "Intelligent optimal control of robotic manipulators using neural networks," *Automatica*, vol. 36, no. 9, pp. 1355–1364, 2000.

[16] N. Cobanoglu, E. Tatlicioglu, and E. Zergeroglu, "Neural network based repetitive learning control of robot manipulators," in *Proc. Amer. Control Conf.*, Seattle, WA, USA, 2017, pp. 5318–5323.

[17] D. M. Dawson, M. M. Bridges, and Z. Qu, *Nonlinear Control of Robotic Systems for Environmental Waste and Restoration*. Englewood Cliffs, NJ, USA: Prentice-Hall, 1995.

[18] J. Nakanishi, R. Cory, M. M. J. Peters, and S. Schaal, "Operational space control: A theoretical and empirical comparsion," *Int. J. Robot. Res.*, vol. 27, no. 6, pp. 737–757, 2008.

[19] F. L. Lewis, D. M. Dawson, and C. T. Abdallah, *Robot Manipulator Control: Theory and Practice*. New York, NY, USA: Marcel Dekker, 2003.

[20] F. L. Lewis, C. T. Abdallah, and D. M. Dawson, *Control of Robot Manipulators*. New York, NY, USA: MacMillan, 1993.

[21] Y. H. Kim and F. L. Lewis, *High-Level Feedback Control With Neural Networks*. Singapore: World Sci., 1998.

[22] F. L. Lewis, S. Jagannathan, and A.Yesildirek, *Neural Network Control of Robot Manipulators and Nonlinear Systems*. London, U.K.: Taylor & Francis, 1999.

[23] K. Hornik, M. Stinchcombe, and H. White, "Multilayer feedforward networks are universal approximators," *Neural Netw.*, vol. 2, no. 5, pp. 359–366, 1989.

[24] M. Krstic, I. Kanellakopoulos, and P. Kokotovic, *Nonlinear and Adaptive Control Design*. New York, NY, USA: Wiley, 1995.

[25] E. Zergeroglu and E. Tatlicioglu, "Observer based output feedback tracking control of robot manipulators," in *Proc. Multi Conf. Syst. Control*, Yokohama, Japan, 2010, pp. 602–607.

[26] V. Stepanyan and A. Kurdila, "Asymptotic tracking of uncertain systems with continuous control using adaptive bounding," *IEEE Trans. Neural Netw.*, vol. 20, no. 8, pp. 1320–1329, Aug. 2009.

[27] B. Bidikli, E. Tatlicioglu, E. Zergeroglu, and A. Bayrak, "An asymptotically stable continuous robust controller for a class of uncertain MIMO nonlinear systems," *Arxiv e-prints*, Jan. 23, 2013. [Online]. Available: https://arxiv.org/abs/1301.5483

[28] B. T. Costic, M. S. de Queiroz, and D. M. Dawson, "A new learning control approach to the active magnetic bearing benchmark system," in *Proc. Amer. Control Conf.*, Chicago, IL, USA, 2000, pp. 5989–5994.

[29] Y. Fang, M. G. Feemster, D. M. Dawson, and N. Jalili, "Nonlinear control techniques for the atomic force microscope system," in *Proc. ASME Int. Mech. Eng. Congr.*, New Orleans, LA, USA, 2002, pp. 1–8.